FOLIA MEDICA CRACOVIENSIA
Vol. LVIII, 4, 2018: 5–12
PL ISSN 0015-5616
DOI: 10.24425/fmc.2018.125699

Printable 3D model of the sella turcica region including the interclinoid bridge

Janusz Skrzat[1], Anna Bonczar[2], Tomasz Kasprzycki[3]

[1]Department of Anatomy, Jagiellonian University, Medical College, Kraków, Poland
[2]Clinic of Ophthalmology, K. Gibiński University Clinical Center, Katowice, Poland
[3]Faculty of Medicine, Jagiellonian University, Medical College, Kraków, Poland

Corresponding author: Janusz Skrzat, PhD, DSc
Department of Anatomy, Jagiellonian University Medical College
ul. Kopernika 12, 31-034 Kraków, Poland
Phone/Fax: +48 12 422 95 11; E-mail: j.skrzat@uj.edu.pl

Abstract: The objective of the study was to create a printable 3D model of the sellar region of the sphenoid bone for demonstrating anatomical variant of the osseous bridging between anterior and posterior clinoid processes. Three-dimensional reconstruction of the middle cranial fossa along with 3D printed model, allow for accurate depicting position of the interclinoid bridge with reference to other basicranial structures.

Key words: 3D reconstruction, sphenoid bone, sellar region, interclinoid bridges.

Introduction

Anatomy and variation of the osseous surrounding of the pituitary gland and neurovascular structures passing through the sphenoid bone remain in close relation with their function and clinical meaning. Besides constant anatomical structures of this cranial region, occasionally appears bony trabeculas resulted from ossification of the dural bands stretched between anterior, middle and posterior clinoid processes of the sphenoid bone [1, 2]. These inconstant bony bridges are termed as: interclinoid bridge (between anterior and posterior clinoid processes) and carotico-clinoid

bridge (between the anterior and the middle clinoid processes). Ossification of the interclinoid ligament can compress the oculomotor nerve, and ossified caroticoclinoid ligament may influence on the blood flow in the internal carotid artery [3–5].

The complete or incomplete osseous bridges in the sellar region occur unilaterally or bilaterally with variable incidence which depends on human population. For example, in Turkish population the incidence of interclinoid osseous bridge was found as 8.18%. In turn, in the same population the total incidence of the ossified caroticoclinoid ligament has been estimated as 36.97% [6]. In other human populations incidence of the interclinoid bridges ranges from 1% to 9% [7–9], whereas in Greek individuals, occurrence of the caroticoclinoid bridge reached 60.2% [10]. Hence, craniofacial defects can rise frequency of the of sella turcica bridges, which increases their risk of interfering with the neurovascular structures [11, 12].

The anatomical variants of sellar bridges seems to be relevant for 3D modeling because of their potential clinical significance related with pathologies of the sella turcica and paraclinoid region, which require surgical management aimed on treatment of the paraclinoid aneurysms or removal of tumors located in this cranial region [13–15]. Both virtual and physical 3D models can help plan surgical procedures in such a way which would minimize risk or avoid complications during operation. 3D models can accurately highlight topographical features and individual anatomy of the osseous structures which have to be resected during operation, such as clinoidectomy. Thereby, the aim of this study was to create virtual and printable 3D model of the sellar region for demonstrating its anatomy and variability related to clinical implications.

Materials and Methods

Three-dimensional reconstruction of the sellar region was based on X-ray CT data of the human skull of an adult individual housed in the Department of Anatomy of the Jagiellonian University, Medical College. Both the facial and cranial bones show normal anatomy; however, on the intracranial surface of the sphenoid bone, an inconstant bony bridge connecting the anterior and posterior clinoid processes of the sphenoid bone was observed. Supplementary information about the investigated case can be found in the previously published report [16].

Computed tomography of the investigated skull was performed by Siemens Sensation 10 CT scanner according to the following protocol: head (Iner EarUHR), slice thickness 0.6 mm, voxel dimensions $336 \times 512 \times 512$, kVP 120.

To obtain a three-dimensional representation of the cross section images of the sellar region two different techniques were used: volume and surface renderings. For volumetric and multiplanar reconstructions of the cranial base showing location

of the interclinoid bridge was applied VolView open source software dedicated for medical data visualization (https://www.kitware.com/volview).

Length of the interclinoid bridge and distances to the selected structures of the sphenoid bone were measured on the volumetric reconstruction of the cranial base using RadiAnt DICOM Viewer software (https://www.radiantviewer.com/pl/).

Further, CT data were converted to geometrical primitives (triangles) which approximated the surface of the rendered objects. Created mesh of triangles served to build printable 3D model of the sellar region. For this purpose, we used free medical software — the InVesalius, which generated virtual reconstructions of the cranial base from two-dimensional images acquired by the computed tomography (http://www.cti.gov.br/invesalius).

Results

Multiplanar and volumetric reconstructions of the sellar region revealed anatomical details of the sphenoid bone (not described in this report because of their common appearance depicted in the atlases of human anatomy), and the inconstant bony bridge that was stretched between the anterior and posterior clinoid processes of the left side of the skull (Fig. 1). Distances of the interclinoid bridge to the selected left-sided structures of the sphenoid bone are presented in Fig. 2.

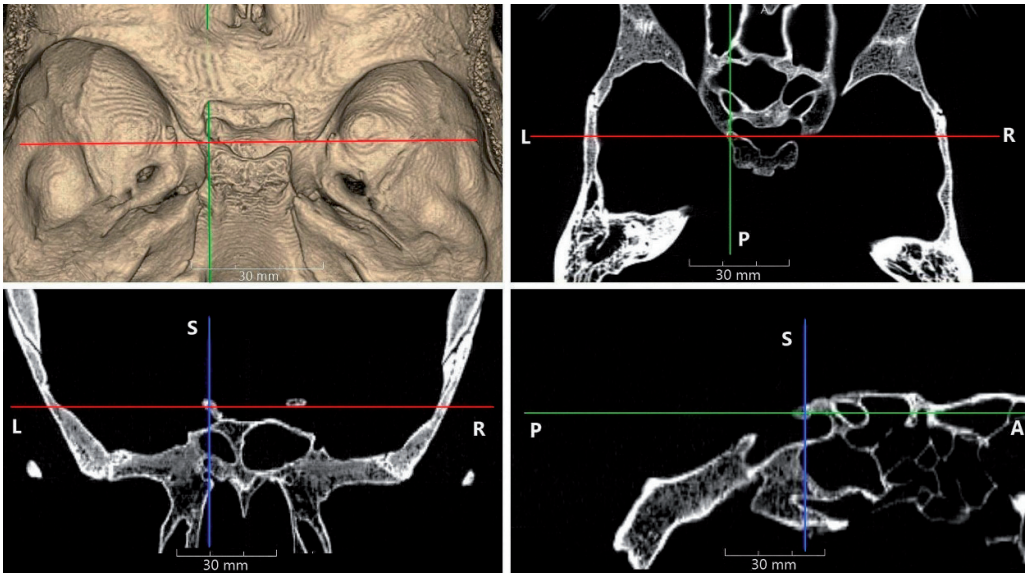

Fig. 1. Volumetric (superior view) and multiplanar reconstructions demonstrating appearance and position of the interclinoid bridge (indicated by the cross-line) in the cranial cavity viewed in the coronal, axial and sagittal planes.

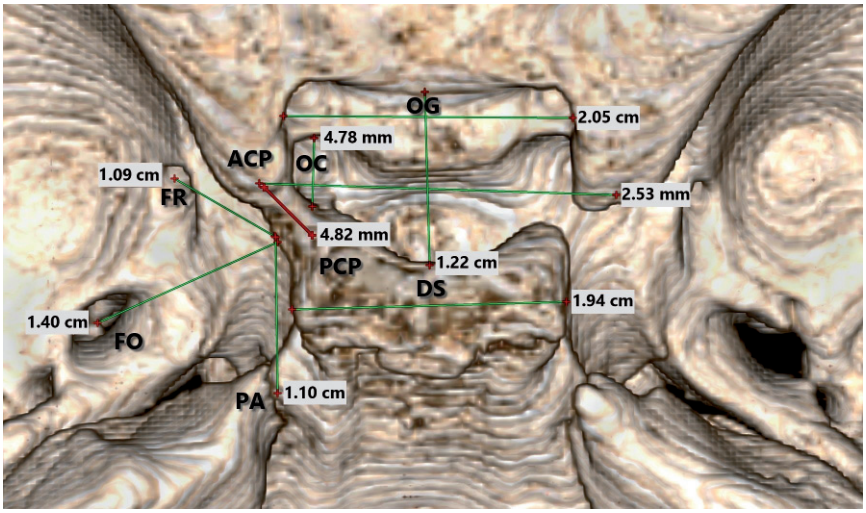

Fig. 2. Measurements of the sellar region (ACP — anterior clinoid process, PCP — posterior clinoid process, OG — optic groove, DS — dorsum sellae), and distances of the interclinoid bridge to the optic canal (OC), foramen rotundum (FR), foramen ovale (FO), and the petrous apex (PA) of the left side.

Created 3D mesh model of the sellar region disclosed morphological appearance of the interclinoid bridge and its location towards other bony structures of the middle cranial fossa as it was presented in volumetric reconstruction (Fig. 3). A significant

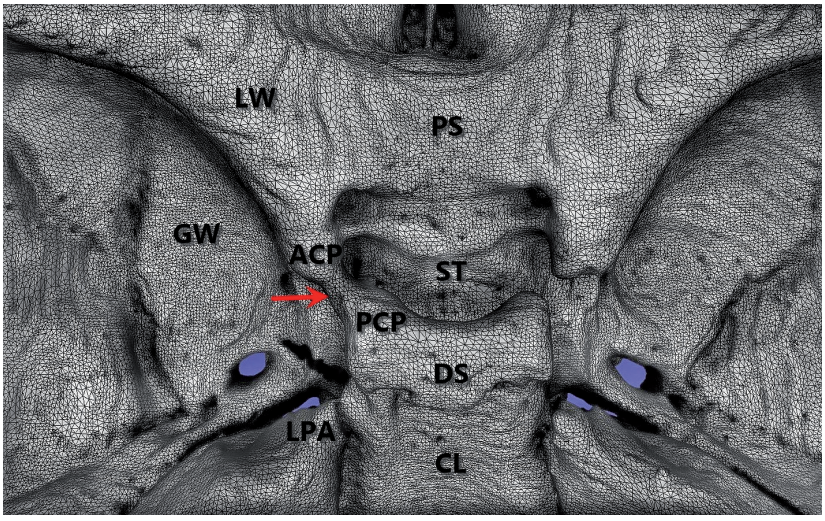

Fig. 3. 3D mesh model of the middle cranial fossa showing sellar region in the superior aspect. On the left side the arrow indicates complete interclinoid bridge; ACP — anterior clinoid process, PCP — posterior clinoid process. LW — lesser wing of sphenoid bone, GW — greater wing of sphenoid bone, PS — planum sphenoidale, ST — sellae turcica, DS — dorsum sellae, CL — clivus, LPA — left petrous apex.

benefit of the created 3D mesh model was the possibility of visual exploration of anatomical relationship in close-up views and at different angles without loss of visual information, contrary to the volumetric reconstruction. With increase of magnification, the volumetric model becomes blurred and more difficult to view. Thus, we could also observe anatomy and arrangement of the osseous structures from above, medial and lateral aspects focused on the fusion patterns between clinoid processes (Fig. 4A). Close-up observation of the interclinoid bridge revealed the presence of a short bony trabecula supporting the middle part of the interclinoid bridge. This pillar limited posteriorly the passage for the left internal carotid artery, thus a part of the carotid sulcus was converted into a foramen (Fig. 4B).

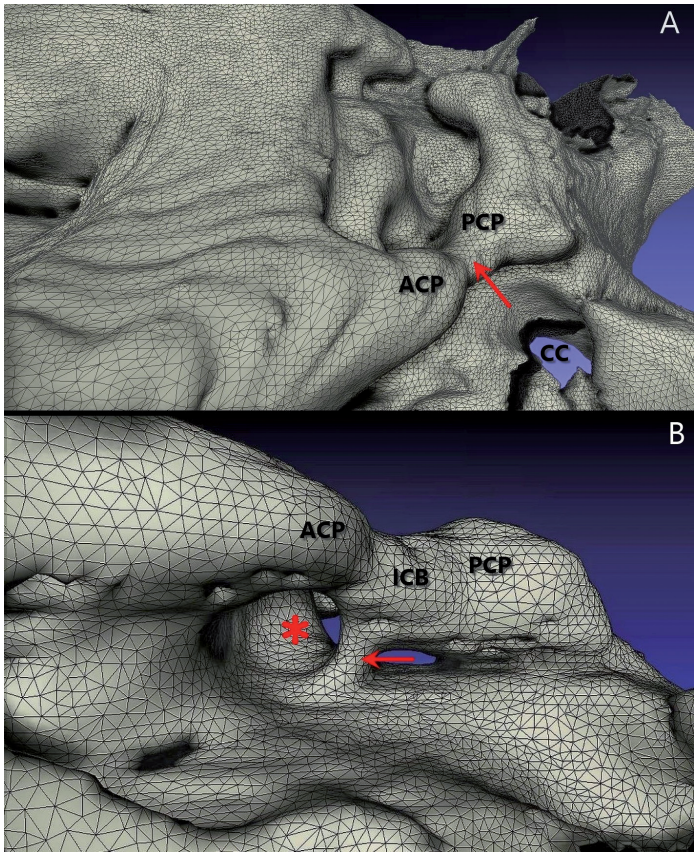

Fig. 4. 3D mesh model of the sellar region. A close-up of the interclinoid bridge (indicated by arrow in A) seen in the latero-superior (A) and lateral (B) projections. Also visible osseous pillar (indicated by arrow in B) supporting the middle part of the interclinoid bridge. This pillar limits posteriorly the passage for the left internal carotid artery, thus the carotid sulcus was converted into the foramen (marked by asterix) located underneath the left anterior clinoid process; ACP — anterior clinoid process, PCP — posterior clinoid process, ICB — interclinoid bridge, CC — carotid canal.

3D model of the sellar region gave opportunity to perform measurements of the interclinoid bridge and related bony structures. We found the length of the interclinoid bridge to be 4.8 mm, however end-to-end measuring points located on the anterior and the posterior clinoid processes were set with approximation because their tips were joined by the continuous osseous bar. In such a case, we demarcated the measuring points on the clinoid processes of the left side according to corresponding tips of the clinoid processes of the right side. The height of the pillar supporting the interclinoid bridge was measured as 1.8 mm, whereas diameters of the foramen transmitting the carotid artery were measured as 4.9 × 5.0 mm.

Discussion

The sella turcica region and related neurovascular structures have been extensively examined because of their clinical importance. Clinical anatomy of this cranial region plays a crucial role for planning surgical treatment of the pituitary tumors and other lesions which may afflict the middle cranial fossa. Therefore, pathological features of the sellar and parasellar regions were the scope of different investigating techniques comprising imaging based on computed tomography, magnetic resonance and endoscopic observation [17, 18]. Morphological variability of the sellar region may be caused by age-related changes (normal physiological processes), or by developmental disturbances related with craniofacial deviations or pituitary fossa pathologies [11, 19]. Numerous anatomical variants of the sphenoid bone, as well as incidence of inconstant bony bridges, resulted from ossification of the dura matter bands were previously described in literature [2–7, 20–22]. As mentioned in the introduction complete or incomplete, unilateral or bilateral bridging between anterior and posterior clinoid processes has been observed with variable frequencies. However, their presence can be disadvantageous for surgical procedures using the transsphenoidal approach to the cranial cavity [23]. Therefore, sphenoid region of the human skull requires building of three-dimensional models for better visualization of its anatomy, simulation of preoperative planning and demonstrating dysmorphologies of the cranial bones. This is mainly caused by anatomical complexity related with occurrence of various inconstant bony structures within the sellar region.

Recent advances in 3D printing technologies have given strong support for demonstrating anatomical structures in details. Rapid manufacturing of replicas, encourages more precise surgical strategies on the physical 3D models, and to transfer these skills into real life skull base surgery.

In this case, creation of anatomical models becomes relatively quick and inexpensive [24–25]. This is particularly beneficial for demonstrating various dismorphologies or congenital anomalies which need surgical intervention [26–27].

The current study presented a case of anatomical variation which can be materialized as a 3D model by 3D printing and used for demonstrating clinical aspects related to sphenoid bone morphology. The 3D virtual models of anatomical variants can provide researchers unlimited possibilities of conducting comparative studies and facilitate insight into specimens which have been presented previously only on photographs. Accessibility to the virtual anatomical collections give opportunity not only to observe anatomical features from different angles (rotate the model), but also interactively enlarge the specimen which enhances visual inspection of morphological details. Regarding above-mentioned aspects, creation and propagation of virtual datasets via the web can deliver valuable information about variation of the anatomical structures in relatively short time, and discuss them on the internet forum.

Conclusions

Created 3D model of the middle cranial fossa showed anatomical variant of the bony bridging found unilaterally in the sellar region between the anterior and posterior clinoid processes. The virtual model can be displayed on the computer screen in close-up for demonstrating anatomical details of the sellar region, either materialized by 3D printing for simulating surgical approaches to the paraclinoid region regarding inconstant bony bridge.

Conflict of interest

None declared.

References

1. *Chin B.M., Orlandi R.R., Wiggins R.H.*: Evaluation of the sellar and parasellar regions. Magn Reson Imaging Clin N Am. 2012; 20 (3): 515–543. doi: 10.1016/j.mric.2012.05.007.
2. *Galdames I.C.S., Matamala D.A.Z., Smith R.L., Suazo G., Zavando M., Smith R.*: Ossification of the sella turcica and clinoid ligments, case report, morphological study and literature review. Int J Morphol. 2008; 26 (4): 799–801.
3. *Ozdogmus O., Saka E., Tulay C., Gurdal E., Uzun I., Cavdar S.*: Ossification of interclinoid ligament and its clinical significance. Neuroanatomy. 2003; 2 (1): 25–27.
4. *Pal M., Sangma G.T.N.*: The Ossified Caroticoclinoid Ligament and Interclinoid Ligament in a Specimen of Sphenoid Bone: A Case Report. Sch J App Med Sci. 2014; 2: 633–635.
5. *Peker T., Karaköse M., Anil A., Turgut H.B., Gülekon N.*: The incidence of basal sphenoid bony bridges in dried crania and cadavers: their anthropological and clinical relevance. Eur J Morphol. 2002; 40 (3): 171–180. PMID: 14566610.
6. *Erturk M., Kayalioglu G., Govsa F.*: Anatomy of the clinoidal region with special emphasis on the caroticoclinoid foramen and interclinoid osseous bridge in a recent Turkish population. Neurosurg Rev. 2004; 27 (1): 22–26. doi: 10.1007/s10143-003-0265-x.

7. *Cederberg R.A., Benson B.W., Nunn M., English J.D.*: Calcification of the interclinoid and petroclinoid ligaments of sella turcica: a radiographic study of the prevalence. Orthod Craniofac Res. 2003; 6 (4): 227–232. PMID: 14606526.
8. *Archana R., Anita R., Jyoti C., Punita M., Rakesh D.*: Incidence of osseous interclinoid bars in Indian population. Surg Radiol Anat. 2010; 32 (4): 383–387. doi: 10.1007/s00276-009-0582-z.
9. *Azeredo R.A., Libreti F.A., Watanabe I.S.*: Anatomical variations of the clinoid process of the human sphenoid bone. Arq Cent Estud Curso Odontol. 1988–1989; 25–26 (1–2): 5–11. PMID: 3275175.
10. *Natsis K., Piagkou M., Lazaridis N., Totlis T., Anastasopoulos N., Constantinidis J.*: Incidence and morphometry of sellar bridges and related foramina in dry skulls: Their significance in middle cranial fossa surgery. J Craniomaxillofac Surg. 2018; 46 (4): 635–644. doi: 10.1016/j.jcms.2018.01.008.
11. *Becktor J.P., Einersen S., Kjaer I.*: A sella turcica bridge in subjects with severe craniofacial deviations. Eur J Orthod. 2000; 22: 69–74. PMID: 10721247.
12. *Sobuti F., Dadgar S., Seifi A., Musavi S.J., Hadian H.*: Relationship between bridging and dimensions of sella turcica with classification of craniofacial skeleton. Pol J Radiol. 2018; 83: 120–126. doi: 10.5114/pjr.2018.76153.
13. *De Jesus O., Sekhar L.N., Riedel C.J.*: Clinoid and paraclinoid aneurysms: surgical anatomy, operative techniques, and outcome. Surg Neurol. 1999; 51: 477–487. PMID: 10321876.
14. *Kim J.M., Romano A., Sanan A., van Loveren H.R., Keller J.T.*: Microsurgical anatomic features and nomenclature of the paraclinoid region. Neurosurgery. 2000; 46 (3): 670–682. PMID: 10719864.
15. *Zhang Y., Yang W., Zhang H., Liu M., Yin X., Zhang L., Cheng K., Nan G., Li Y.*: Internal Carotid Artery and its Relationship with Structures in Sellar Region: Anatomic Study and Clinical Applications. World Neurosurg. 2018; 110: e6–e19. doi: 10.1016/j.wneu.2017.09.145.
16. *Skrzat J., Szewczyk R., Walocha J.*: The ossified interclinoid ligament. Folia Morphol. (Warsz). 2006; 65 (3): 242–245. PMID: 16988924.
17. *Naidich M.J., Russell E.J.*: Current approaches to imaging of the sellar region and pituitary. Endocrinol Metab Clin N Am. 1999; 28 (1): 45–79. PMID: 10207685.
18. *Neubauer A., Wolfsberger S., Forster M.T., Mroz L., Wegenkittl R., Buhler K.*: Advanced virtual endoscopic pituitary surgery. IEEE Trans Vis Comput Graph. 2005; 11 (5): 497–507. PMID: 16144247.
19. *Shah L.M., Phillips C.D.*: Imaging sellar and suprasellar pathology. *Appl Radiol.* 2009; 38 (4): 9–21.
20. *Skrzat J., Mróz I., Marchewka J.*: Bridges of the sella turcica — anatomy and topography. Folia Med Cracov. 2012; 52 (3–4): 97–101. PMID: 24852690.
21. *Skrzat J., Kozerska M., Wróbel A.*: Micro-computed tomography study of the abnormal osseous extensions of sella turcica. Folia Morphol. (Warsz). 2014; 73 (1): 19–23. doi: 10.5603/FM.2014.0003.
22. *Zdilla M.J., Cyrus L.M., Lambert H.W.*: Carotico-clinoid foramina and a double optic canal: A case report with neurosurgical implications. Surg Neurol Int. 2015; 6: 13. doi: 10.4103/2152-7806.150456.
23. *Rhoton A.L. Jr, Harris F.S., Renn W.H.*: Microsurgical anatomy of the sellar region and cavernous sinus. Clin Neurosurg. 1977; 24: 54–85. PMID: 583699.
24. *McMenamin P.G., Quayle M.R., McHenry C.R., Adams J.W.*: The production of anatomical teaching resources using three-dimensional (3D) printing technology. Anat Sci Educ. 2014; 7 (6): 479–486. doi: 10.1002/ase.1475.
25. *Vaccarezza M., Papa V.*: 3D printing: a valuable resource in human anatomy education. Anat Sci Int. 2015; 90 (1): 64–65. doi: 10.1007/s12565-014-0257-7.
26. *Lopez C.D., Witek L., Torroni A., Flores R.L., Demissie D.B., Young S., Cronstein B.N., Coelho P.G.*: The role of 3D printing in treating craniomaxillofacial congenital anomalies. Birth Defects Res. 2018; 110 (13): 1055–1064. doi: 10.1002/bdr2.1345.
27. *Wang S.S., Zhang S.M., Jing J.J.*: Stereoscopic virtual reality models for planning tumor resection in the sellar region. BMC Neurol. 2012; 12 (1): 146. doi: 10.1186/1471-2377-12-146.